The Journal of the Oceanological Society of Korea
Vol. 27, No. 4, pp. 290-302, December 1992

Observed and Simulated Seasonal Salinity in the Tropical Atlantic Ocean, and its Relationship with Freshwater

JUNG-MOON YOO
Department of Science Education Ewha Womans University Seoul, Korea

관측과 모델에서 얻어진 열대 대서양에서의 계절별 염분 분포 및 담수 효과

유 정 문
이화여자대학교

Seasonal variations of salinity in the upper 500 m of the tropical Atlantic Ocean are examined, based on both climatological seasonal salinity observations and numerical simulations with hydrological forcing. The seasonal cycle of sea surface salinity has strong seasonal variations caused by shifts of the freshwater surplus zone (i.e. the intertropical convergence zone) and the river outflow. The climatological seasonal salinity in this analysis concurs with other independent observations described by Defant (1981) and Levitus (1982), but provides more consistent patterns with temperature structure. The effect of salinity on density below 100 m depth in the tropical Atlantic is negligible compared to that of temperature, while in the mixed layer salinity affects density significantly. The systematic difference between observed and simulated salinity is found to be the fact that the simulated salinity is higher in the tropics but lower in the subtropics than the observed salinity, and possible sources about the difference are also discussed.

기후학적인 관측자료와 담수 효과를 고려한 수치실험에서 얻어진 두가지의 계절별 염분 분포를 열대 대서양 500 m 상층부에 대하여 조사하였다. 해표면 염분의 계절 변화는 담수의 초과를 가져오는 열대수렴대 (ITCZ) 의 이동 및 강물 방출 시기에 밀접한 관계가 있었다. 본 연구에서 얻어진 계절별 염분 분포는 Defant (1981) 와 Levitus (1982) 등의 이미 존재하는 기후 자료와 대체로 비슷하나, 본 연구의 자료가 온도 분포에 더 잘 일치하였다. 밀도에 대한 온도 효과와 비교할 때 염분 효과는 100 m 이심에서는 무시할 만하나 혼합층에서 염분 효과는 상당히 중요하였다. 관측된 염분 분포와 모델에서 계산된 염분 분포사이에 뚜렷한 차이가 염분값의 위도에 따른 기울기에서 나타났다. 모델에서 유도된 염분은 관측값보다 적도부근의 해양에서 대체로 높게 나타났으나, 아열대 해역에서는 낮게 나타났다. 남동 대서양 해역과 같은 관측자료가 매우 적은 곳에서 염분 차이는 크게 나타났고, 이런 해역에서 정교한 모델값이 좀 더 정확한 듯 보인다. 또한 관측값과 모델에서 얻어진 값과의 불일치에 대한 가능한 원인들도 분석하였다.

INTRODUCTION

Recently increasing attention has been drawn to the salinity distribution and budget due to the role of the ocean in the earth's climate through thermohaline circulation and interhemispheric water mass exchanges. The salinity change at the sea surface affects the penetrative convection through its influence on the buoyancy flux. In addition, the most significant effects in the mixed layer produced by the salinity budget are the reduction of the deepening rate and the corresponding changes

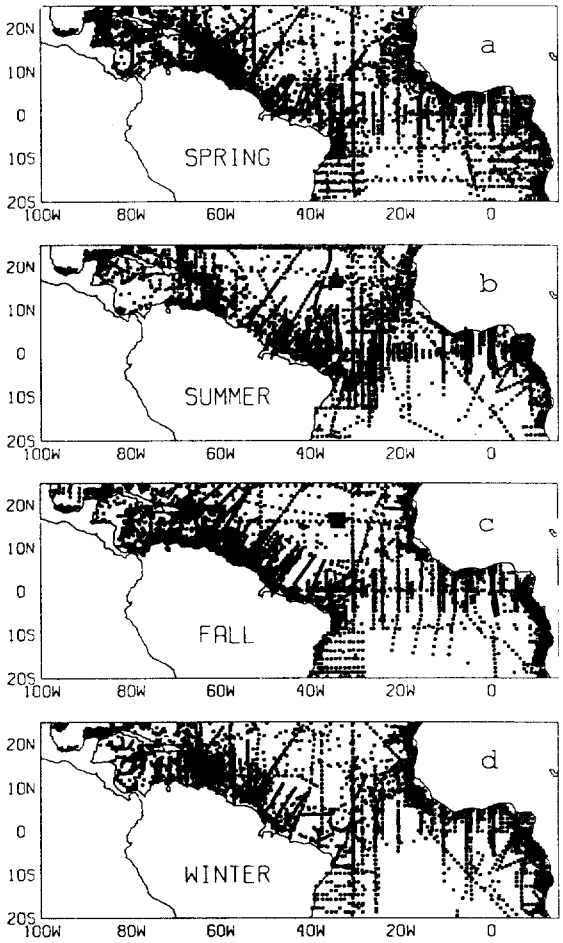

Fig. 1. Distribution of salinity observations from surface to 500 m depth for the tropical Atlantic for (a) spring (March, April and May), (b) summer (June-August), (c) fall (September-November), and (d) winter (December-February).

in the temperature of the mixed layer (Miller, 1976), and thus are important in the climate.

Although the analyses of climatological seasonal salinity data in the tropical Atlantic 20°S-20°N are available in earlier studies (Levitus, 1986; Dessler and Donguy, personal communication), the poor data coverage, for instance, in the southern hemispheric region of the ocean is the primary source of uncertainty (Fig. 1, discussed later). Depending upon how the salinity data are analyzed, various answers can be expected. These conditions preclude the analyses of salinity satisfactorily on a large scale basis.

Over the data sparse regions, a sophisticated ocean general circulation model (see e.g. Philander and Pacanowski, 1986a, 1986b) may provide more reliable salinity output than that obtained from simple objective analysis, if both the realistic model and the accurate initial, input data are given. Based on the relationship between the salinity balance and the freshwater balance, one of the important initial data which drive the model is the surface freshwater flux, which is computed from evaporation minus precipitation (E-P) and river runoff. Unfortunately, both evaporation and precipitation over the tropical Atlantic have been poorly known on a monthly or seasonal basis.

In the tropical Atlantic study, Yoo and Carton (1988, 1990) have estimated precipitation from satellite-derived outgoing longwave radiation data and the height of the base of the trade-wind inversion, applying the precipitation to seasonal freshwater budgets. They also obtain the evaporation and river discharge from several climatological data sources. Following Yoo and Carton (1988, 1990), the seasonal cycle of freshwater flux in the same area has strong annual and semiannual variations caused by shifts of the intertropical convergence zone (ITCZ).

In this paper, we show that more accurate climatological seasonal salinity estimates in the tropical Atlantic Ocean can be obtained with the help of the ocean model, which is forced by the above freshwater data. This paper also presents the new results of the seasonal salinity fields for the tropical Atlantic, obtained from the National Oceanographic Data Center (NODC).

After reviewing the analysis procedure for both the observed salinity and the model output in section 2, we describe annual and semiannual cycle of salinity in section 3 to show the surface freshwater effect on salinity, and the difference between the observed and model salinity. In section 4, we present seasonal zonal-mean salinity fields, averaged from surface to 500 m depth.

OBSERVATION AND SIMULATION

Here we describe how observed and simulated

salinity climatologies have been constructed from historical salinity data and from a numerical simulation in the tropical Atlantic, respectively.

Data analysis

Salinity data 20°S-25°N has been obtained from the NODC for the period 1900 to 1986. The fewest observations have been collected in boreal winter (Figs. 1a-d). The number of full vertical profiles ranges from 9400 in winter to 19100 in summer. The results must be viewed with caution in data-sparse regions, for instance, the South Atlantic in winter. These data counts are about 30 % larger than the data in the widely used analysis of Levitus (1982). The data in that analysis was restricted to the period prior to 1977.

The procedures for the construction of seasonal salinity in our study are as follows: first, we interpolate the salinity data to the depths from the surface to 500 m depth at 14 NODC standard levels (0, 10, 20, 30, 50, 75, 100, 125, 150, 200, 250, 300, 400 and 500 m). However, if the observations of a salinity profile do not include any observed value below 500 m depth, the whole profile is discarded. The data are then composited into seasonal mean values in 1°×1° boxes. Secondly, the salinity differences between seasonal NODC observations and Levitus' annual average salinity are computed. This means that Levitus' annual salinity is used as a first-guess. We analyze the salinity differences using statistical objective analysis. In the analysis, a correction to the first-guess at each gridpoint is computed based on an optimal weighting of data surrounding the gridpoint. The weighting depends inversely on the distance between the gridpoint and the surrounding gridpoints (see Haltiner and Williams, 1980) with a correction scale of 400 km. Thus, the analyzed value at the gridpoint is the sum of the first guess value and the difference. Lastly, by adding Levitus' annual estimate back to the objectively analyzed salinity differences, we reconstruct our estimated seasonal salinity fields on a 1°×1° grid at the 14 standard levels.

It is well-known that the determination of the vertical salinity (S) distribution on the basis of the available observations is more difficult than in the case of temperature (T), and that temperature is well correlated with salinity below the mixed layer. We have tried to improve the analysis of salinity by using the local T-S relationship in combination with Levitus' (1982) seasonal temperature to provide an improved first guess. Comparison of our

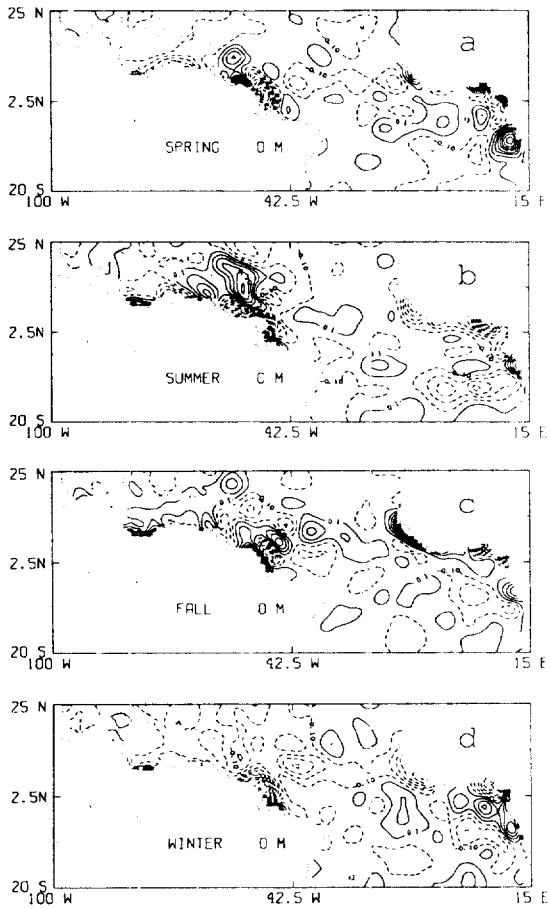

Fig. 2. Levitus' (1982) seasonal mean minus our seasonal mean surface salinity field (‰) for (a) spring, (b) summer, (c) fall, and (d) winter. The definition for seasons is the same as that of Fig. 1. Note that Levitus has differently defined Northern Hemisphere winter as February-April, spring as May-July, summer as August-October and fall as November-January. After we linearly interpolate Levitus' seasonal salinity data into monthly data for the present comparison, we again obtain his seasonal mean salinity using our season definition. Contour interval is 0.2‰, for instance, ± 0.1, ± 0.3, ± 0.5···

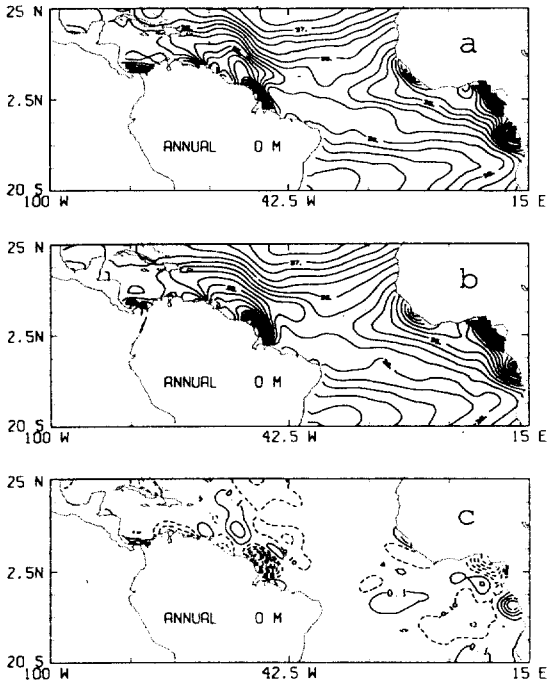

Fig. 3. Annual mean salinity (‰) at the sea surface from (a) this study and (b) Levitus (1982). Contour interval is 0.25‰. (c) Levitus' (1982) annual mean minus our annual mean surface salinity field (‰). Contour interval is 0.2‰, for instance, ±0.1, ±0.3, ±0.5…

analysis of sea surface salinity with Levitus (1982) shows that in our analysis salinities for winter are systematically higher by 0.1-0.5‰ in the region of the ITCZ (Fig. 2). The two annual-mean climatologies at the sea surface agree to within ±0.1‰ except in the areas offshore of the major rivers (Fig. 3), and agree to within ±0.05‰ in the vertical cross-section of zonally averaged salinity as a function of latitude and depth. In the region of strong seasonal variation associated with the North Equatorial Countercurrent, the vertical movement of isohalines is larger in our analysis, more consistent with the motion of isotherms.

Simulation

The primitive equation model used in this study is that of Philander and Pacanowski (1986a) and in detail described in Carton (1991). The model domain extends from 30°S to 50°N with 1°×1/3° resolution equatorward of 10° and coarser resolution at high latitudes. Realistic basin geometry and topography are included. The model is divided into 27 levels in the vertical, with 10 m spacing in the upper 100 m. Initial conditions for these experiments are provided by Levitus (1982), while seasonal wind forcing is provided by Hellerman and Rosenstein (1983). Horizontal mixing and diffusion is specified by a constant eddy coefficient of 2×10^7 cm^2/s. The coefficient of vertical mixing and diffusion are Richardson number dependent following Pacanowski and Philander (1981) with one exception. Under stable conditions the minimum vertical mixing rate Kv of heat and salt under highly stratified conditions was increased to 0.0134 cm^2/s in order to maintain numerical stability. In each experiment the model has been integrated from its initial state for three years, with the analysis carried out in the third year.

Surface heating due to incident solar radiation is assumed to have a constant value corresponding to its climatological average. Sensible and latent heating are estimated from a bulk formula which depends on the air-sea temperature contrast, where climatological seasonal air temperature is specified. Because latent and sensible heating of the atmosphere by the ocean are themselves functions of sea surface temperature (SST), the surface heat flux acts to inhibit changes in SST. Experiments with this heat flux formulation (Carton and Shukla, 1991) give a time scale of this feedback of 75-100 days.

Initial conditions are the climatological monthly temperature and salinity conditions of Levitus (1982). Each simulation is carried out for three seasonal cycles, with the analysis confined to the last seasonal cycle. The model is forced by observed seasonal freshwater flux between 20°S-25°N with the surface boundary condition of freshwater flux. Because the model has a rigid lid, specification of surface freshwater flux is interpreted as a flux of salt through the rigid model surface at a rate which is proportional to the difference between evaporation, precipitation, and river discharge.

$$K_v \frac{\partial S}{\partial Z}(x, y, o, t) = S(x, y, o, t) \times (E\text{-}P\text{-}R)$$

where S (x, y, o, t) is salinity, E is evaporation, P is precipitation and R is river discharge. River discharge is interpreted as a concentrated area of precipitation occurring uniformly in a 2°×2° area nearest the actual location of the river mouth. In the case of rivers with multiple distributaries, like the Amazon, the discharge area is centered on the average point of discharge. In the following section we compare the annual and semiannual cycles of simulated salinity with those of observed values in the layer between sea surface and 100 m depth.

SEASONAL CYCLE OF THE SURFACE-LAYER FRESHWATER AND SALINITY

The surface-layer salinity in a given basin is affected by surface freshwater flux, and by water that is flowing into and out of the basin by advection and/or diffusion (and by the local storage on seasonal time scale). Thus, comparison of the distributions of both freshwater flux and salinity in the surface-layer can show predominant physical processes in the calculation of the mixed layer. In this section we first introduce the behavior of observed freshwater flux, used to force the model. Then we compare the annual and semiannual cycles of simulated salinity with those of observed values in the layer between sea surface and 100 m depth, which approximately corresponds to the mixed layer in the tropical Atlantic.

Surface freshwater flux

Monthly surface freshwater flux for the tropical Atlantic is available in Yoo and Carton (1990), who obtain the flux by combining estimates of evaporation (Oberhuber, 1988), precipitation (Yoo and Carton, 1988), and river discharge (UNESCO, 1969, 1971a, b, 1978, 1979) (Fig. 4 and Table 1). Since the intertropical convergence zone (ITCZ) in which much of the freshwater surplus due to heavy rainfall takes place, undergoes strong seasonal shifts, one can expect similarly strong seasonal changes in the sea surface salinity (Figs. 4 and 6). In this region the seasonal downward moisture flux (i.e. E-P<0) is about 9-27 cm/month, while in the northern and southern subtropics the upward moisture flux (i.e. E-P>0) is about 9-15 cm/month. Inclusion of river runoff enhances the zonally averaged freshwater flux by up to 8 cm /month. We can also anticipate the strong seasonal variations and lowest values in the sea surface salinity near the mouths of large rivers.

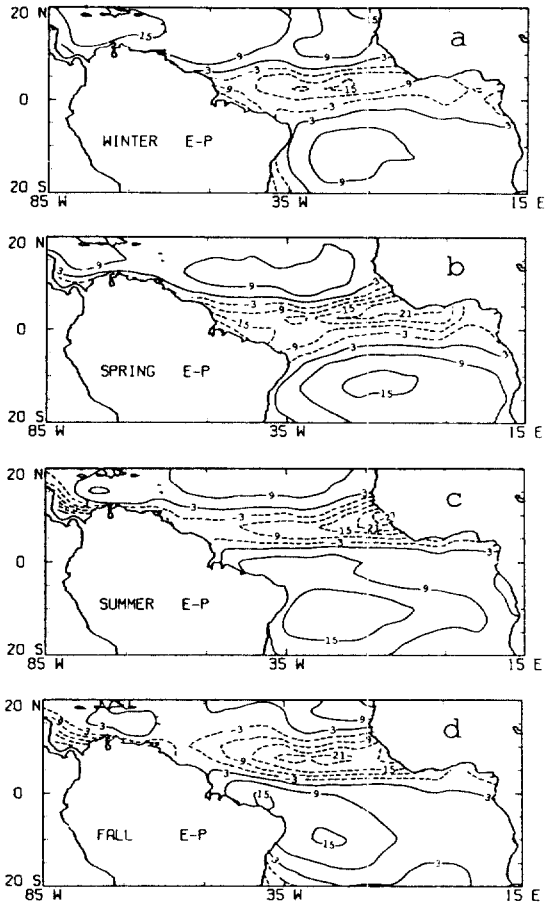

Fig. 4. Climatological moisture balance (E-P) distribution from Yoo and Carton (1990) for (a) winter (December-February), (b) spring (March-May), (c) summer (June-August), and (d) fall (September-November). Contour interval is 6 cm/month. Negative values indicate the excess amounts of precipitation over evaporation.

Table 1. Monthly discharge from the nine largest tropical Atlantic rivers with the Mississippi, in units of 10^3 m^3/s.

River	Jan	Feb	Mar	Apr	May	Jun	Jul	Aug	Sep	Oct	Nov	Dec
Amazon (0°N, 49°W)	116	145	171	195	211	211	199	174	137	103	93	98
Congo (6°S, 13°E)	46	38	34	36	38	35	30	32	38	46	54	56
Mississippi (29°N, 89°W)	40	46	49	59	60	42	30	21	19	22	26	35
Orinoco (9°N, 61°W)	12	7	6	7	15	28	43	54	59	52	37	25
Ogooue (1°S, 9°E)	5	4	5	6	6	5	3	2	2	4	8	7
Niger (5°N, 6°E)	5	4	2	1	0	1	2	6	10	11	8	6
Sao Francisco (11°S, 37°W)	5	5	5	4	3	2	2	1	1	1	2	3
Volta (6°N, 16°W)	0	0	0	0	0	0	1	2	4	4	1	0
Senegal (16°N, 17°W)	0	0	0	0	0	0	0	2	2	1	0	0

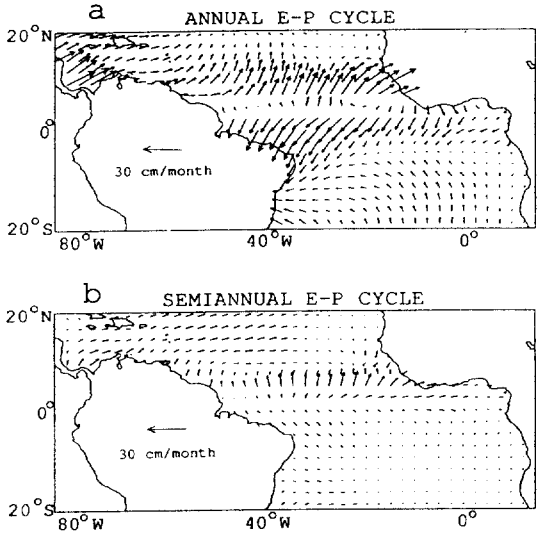

Fig. 5. Normalized amplitude and phase of the moisture balance over the tropical Atlantic Ocean from Yoo and Carton (1990). (a) Mean annual cycle, (b) mean semiannual cycle. Normalized amplitude is indicated by the length of the arrows. Phase is indicated by the orientation of the arrow. Arrows indicating maximum of the moisture balance on January 1 point north and rotate clockwise about 1° per day so that a 90° phase angle of 1 April vector points eastward.

The annual cycle of evaporation minus precipitation due to the bulk of rainfall caused by the movement of the ITCZ is stronger in the region between 5°S and 10°N than in the other region (Fig. 5a). In the Caribbean Sea, the annual signal is even stronger because there is a substantial freshwater deficit throughout the year, except a slight freshwater surplus in fall. The semiannual cycle is large in the region near the annual mean position (~5°N) of the ITCZ because of the double passage of the ITCZ in spring and fall, respectively (Fig. 5b). As a result, the seasonal cycle of freshwater flux in the tropical Atlantic has strong annual and semiannual variations caused by shifts of the intertropical convergence zone (ITCZ). According to Yoo and Carton (1990), the error in the freshwater flux is one-third of the freshwater flux itself.

Monthly mean river runoff rate to the tropical Atlantic has been obtained from UNESCO for nine major rivers between 20°S and 25°N, including the Mississippi river which discharges into the Gulf of Mexico (Table 1). The Amazon river provides 65 % of total annual mean runoff rate of 2.37×10^5 m^3/s into the tropical Atlantic. The Amazon transports vary with maximum (2.1×10^5 m^3/s) in May-June and minimuim (0.9×10^5 m^3/s) in November. The Congo and Orinoco rivers provide another 29 %.

Observed salinity

The distribution of seasonal salinity at the sea surface exhibits a number of large-scale patterns, mainly determined by the freshwater budget (Figs. 6a-d). One example is low salinity tongue in the ITCZ and near the mouths of large rivers. Maxima (~37‰) in the salinity occur in the subtropics where evaporation is high. In fall, which is the most rainy season in the tropical Atlantic, a low salinity tongue occurs in the western and central Atlantic. However, at this time the Amazon water, which is brought eastward by the North

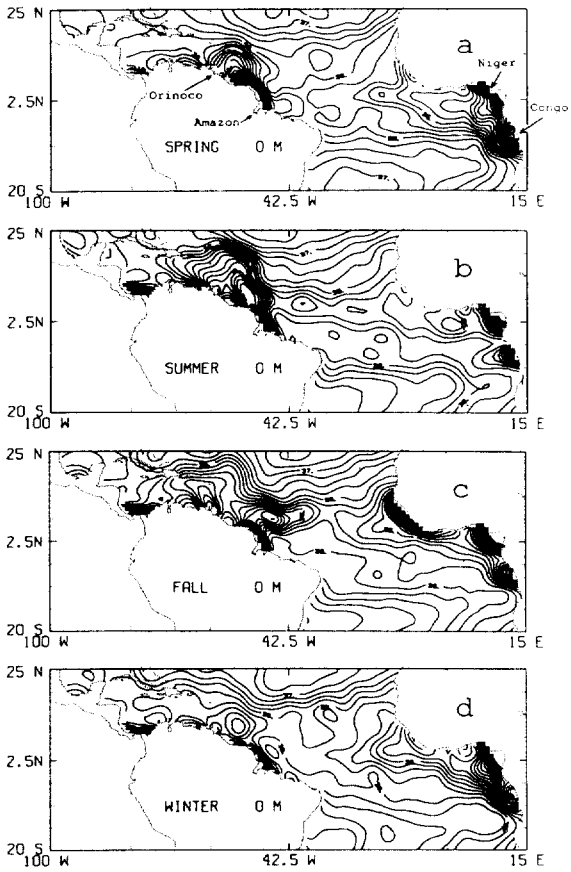

Fig. 6. Observed seasonal mean salinity (‰) at the sea surface for (a) spring, (b) summer, (c) fall, and (d) winter. In Fig. 6, (a) the locations for four of the larger rivers inflowing from the South America and Africa into the tropical Atlantic Ocean are indicated by arrows. The definition for seasons is the same as that of Fig. 1. Contour interval is 0.25‰.

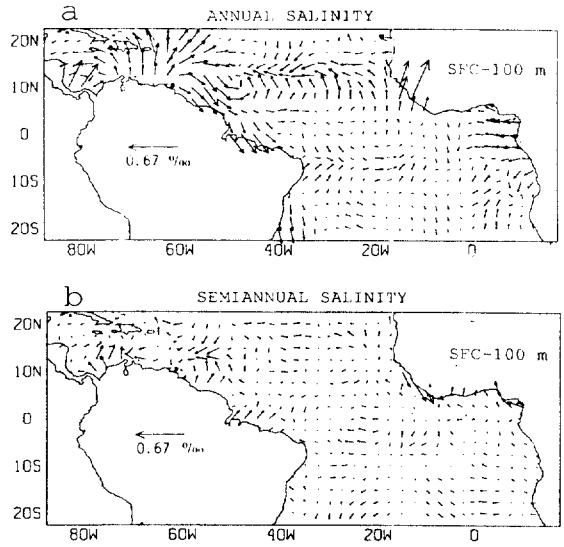

Fig. 7. Normalized amplitude and phase of the observed salinity vertically integrated from surface to 100 m over the tropical Atlantic Ocean. (a) Mean annual cycle, and (b) mean semiannual cycle. Normalized amplitude is indicated by the length of the arrows. The phase convention is the same as in Fig. 5. Unit are ‰.

Equatorial Countercurrent (NECC), also contributes to the low salinity tongue, as recently shown in Coastal Zone Color Scanner images (personal communication, F. Muller-Karger). Large amplitudes of the annual cycle over the open ocean are mostly due to precipitation changes associated with the seasonal movement of the ITCZ.

The annual cycle of the observed salinity vertically integrated from surface to 100 m is strong in the vicinity of the major rivers and in the region, more or less, north of the ITCZ (Fig. 7a). The bands with strong annual variations on either side of about 12°N are almost out of phase with each other. The salinity on the north side of the annual mean position of the ITCZ (about 5°N) is about in phase with the E-P flux, implying that maximum salinity occurs in winter (see also Fig. 5a).

The semiannual signal is irregular and weak except in the coastal areas near major rivers (Fig. 7b and see also Fig. 5b). The discrepancy between the salinity and E-P fields over the open ocean is attributable to other processes besides local storage. Levitus (1986) suggests that advection plays a significant role in the maintenance of the low salinity belt of the subtropics. The model results which show the larger annual variation of salinity are consistent with the influx of E-P in the open ocean, and due to the outflow of the Congo river in the eastern Atlantic (see also Fig. 5a).

One simple way to check whether horizontal advection is unimportant seasonally is to see if river outflow water is stored near the river mouth. On a seasonal basis, area-averaged surface salinity and river discharge correlate significantly (-0.74~-0.99) over the coastal areas of the Amazon, Ori-

Table 2. Correlation coefficients between seasonal river discharge (R) and surface salinity (S) over the coastal areas surrounding four rivers in the tropical Atlantic Ocean. Units of the river discharge and surface salinity are $10^3 m^3 s^{-1}$ and ‰, respectively.

Season	Amazon (53-46W, 1S-5N)		Orinoco (65-62W, 8-11N)		Niger (4-6E, 3-6N)		Congo (6-11E, 8-3S)	
	R	S	R	S	R	S	R	S
Spring	192.3	33.35	9.2	36.51	1.2	32.15	36.1	32.56
Summer	194.6	33.46	41.4	35.63	3.0	33.36	32.1	34.49
Fall	111.1	33.89	49.5	35.14	9.7	30.85	45.8	34.09
Winter	119.8	35.03	14.7	36.27	4.8	31.80	46.8	33.09
Correlation coefficient	−0.74		−0.99		−0.76		−0.19	

noco and Niger rivers (Table 2). A weak correlation in the Congo may be due to both high horizontal advection and flat seasonal cycle of the river discharge compared to those of other three rivers.

The regions with the largest amplitude of the annual cycle are in areas of river runoff (Fig. 7a). The areas offshore of the Amazon and Congo rivers have annual ranges of 3‰ (not shown).

Simulation

The model which is driven by the input data of the Yoo and Carton (1988, 1990) freshwater budget produces estimates of seasonal salinity at 5 m depth generally close to observed salinity values at the corresponding depth (not shown). Maxima (>36.5‰) in the salinity occur in the subtropics of both hemispheres, while minima (<35.5‰) occur in the ITCZ and the areas offshore of the major rivers.

Substracting the values of observed salinity from those of the model at 5 m depth reveals a significant difference (Figs. 8a-d). In the equatorial region between 5°N and 5°S connecting from the Amazon river to the Gulf of Guinea, the seasonal salinity in the model is systematically higher by 0.2-0.6‰ than the observed salinity, but lower by 0.2-0.6‰ in the subtropics. The difference between the two climatologies is also substantially larger in the regions offshore of major rivers. The extreme magnitude of the model minus observed analysis ranges from 3.9‰ near the Amazon river in spring to −1.5‰ at the South Atlantic (6°W, 14°S) in fall.

The above results in the model lead the relative reduction of meridional salinity gradient from the tropics to the subtropics compared to that in the observation. So far we have examined the salinity difference at surface-layer between model and observed values.

The annual cycle of the model salinity estimates vertically integrated from surface to 100 m depth generally agrees with that of observed salinity (Fig. 9a). In both amplitude and phase, the annual cycles of the two climatologies agree well with each other, in particular, in the tropical Atlantic north of the equator, where the observation base is several times as large as south of the equator. However, the belts with strong annual variations on either side of about 12°N shown in observation are shifted northward by about 2.5° in model salinity.

The bands with strong annual variations on either side of about 12.5°N in observed salinity (and of 15°N in model) are out of phase with each other (Figs. 9a and 7a). This implies that two salinity masses, respectively, on the north and south side of the 12.5°N-15°N axis are originated from the different sources and regions. The two salinity masses are as follows; One is the salty outflow which are advected southward from the northern subtropics centered at 25°N, and has a maximum salinity amplitude in summer. The other is the relatively fresh outflow which are advected northward from the ITCZ centered at 5°N, and has a maximum salinity amplitude in winter.

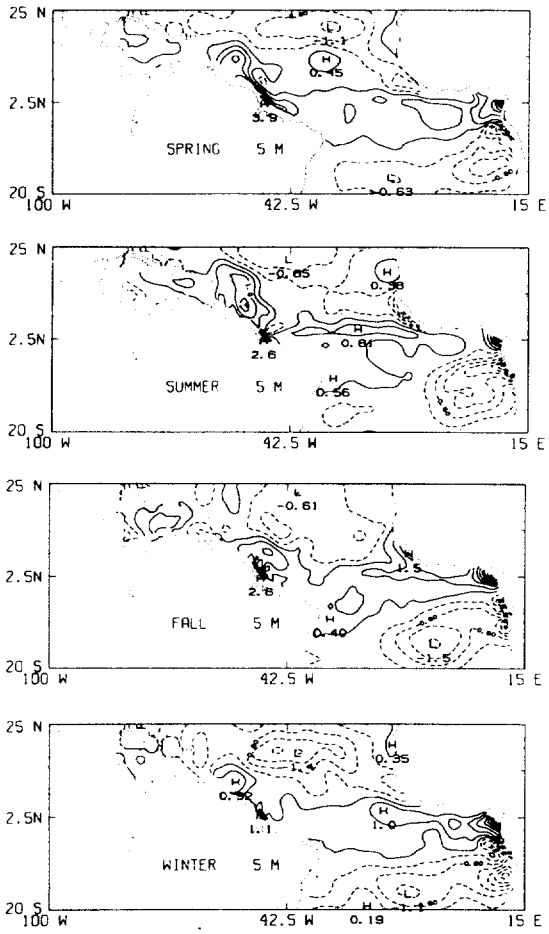

Fig. 8. Simulated seasonal mean minus observed seasonal mean salinity field (‰) at 5 m depth for (a) spring, (b) summer, (c) fall, and (d) winter. The definition for seasons is the same as that of Fig. 1. The observed salinity at 5 m depth is estimated by averaging the salinity values at both sea surface and 10 m depth. Contour interval is 0.4‰, for instance, ±0.2, ±0.6, ±1.0···

The northward horizontal advection of less salty water mass from the ITCZ in model is stronger than in observation, leading the displacement of the axis from 12.5°N to 15°N (Figs. 9a and 7a). The another case which two salinity masses from different sources merge into the zonal belt in the model analysis is also seen near the equator, but not seen in observation. This may be due to the more active equatorial upwelling and undercurrent at about 100 m depth in model than in observation. For the verification and detail analysis of

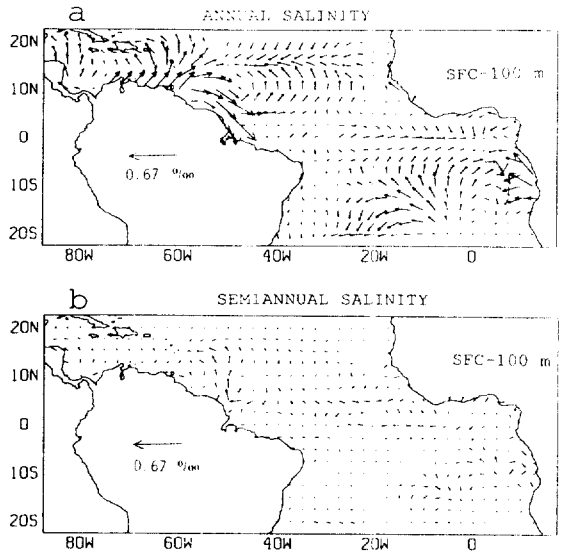

Fig. 9. As in Fig. 7 except for the simulated salinity.

these current results, we need more observations near the equator, particularly in winter (see Fig. 1d).

Moderately strong amplitude in the annual cycle at the equator during early spring occurs in the model, while it is not clear in observed salinity. In addition, there is a significant difference of both amplitude and phase between two climatologies near the African coast at 15°W, 8°N due to coastal upwelling as well as surface freshwater influx.

First of all, however, the largest disagreement in the annual cycles between the model and observed salinity occurs in the central and eastern region of the South Atlantic, where the observed data are sparse (see also Fig. 1). The model results which show the larger annual variation of salinity are consistent with the influx of E-P in the open ocean, and due to the outflow of the Congo river in the eastern Atlantic (see also Fig. 5a). Here the model output seems to be more reasonable than the observed analysis, obtained from the poor data base of observation. At the equator, semiannual signal in model salinity is also obvious in both March and September, but it is somewhat weak in observation (Figs. 9b and 7b).

SEASONAL ZONAL-MEAN SALINITY FROM SURFACE TO 500 M DEPTH

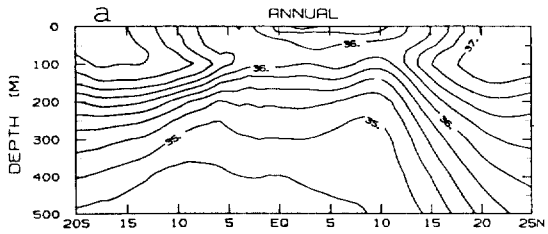

Fig. 10. Observed annual mean salinity (‰), zonally averaged in the region between 30°W and 50°W, as a function of latitude and depth. Contour interval is 0.25‰.

We examine the magnitude and vertical penetration of the annual cycle of salinity, and the vertical structure of various different salinity masses in the tropical Atlantic. In other words, a reason to do this is to see the changes in salinity due to movements of the thermocline.

Observed salinity

The zonally averaged observed salinity fields between 30°W and 50°W in annual mean are presented (Fig. 10). The reason why we investigate the vertical structure of salinity in this area is that the western Atlantic has strong seasonal changes associated with vertical displacements of the thermocline.

The advection of subtropical highly saline water at about the 100 m depth is responsible for the development of the intermediate salinity maximum as observed at the 100-200 m depth in the tropical Atlantic (Fig. 10). The outflow of the saline water maintains about 20-30 m thickness along its entire course without active mixing with the freshwater flux. According to Defant (1936), the maintenance of a very thin water layer unchanged in salinity over large distances is attributed to the stable density stratification at the bottom of the mixed layer, which prevents any mixing with the water mass above and below it. The salinity below 100 m depth tends to decrease from 36‰ to 34.7‰ with increasing depth. Minimum salinity (34.7‰) also occurs in the layer below 400 m depth south of 8°N, while the maxima (>37‰) of the salinity occur at both 20-25°N and 15-20°S above 150 m depth. A local salinity minimum (35.5‰) due to the surface freshwater influx in the ITCZ is also observed in the surface at 2-3°N.

Examining the detail vertical structure in the layer (100-150 m) in the region between the equator and 10°N, the vertical distribution ('V' curve) of our salinity data is consistent with both thermal structure and Defant (1981) (Fig. 10). In other words, the vertical structure of this study in that region provides a more favorable condition for the westward South Equatorial Current (SEC) in 0-5 °N and for the eastward North Equatorial Counter Current (NECC) in 5-10°N under a geostrophic balance, although the SEC is caused mainly by the trade winds and the NECC by the curl of wind stress.

Investigation of the difference fields of observed salinity for each season indicates that the annual cycle of salinity generally extends to 250 m depth, using the 0.1‰ as an indicator of substantial variation in the zonally averaged field of the difference (Figs. 11a-d). However, we note that in the tropical Atlantic the 0.15‰ isoline is found even in the whole layer (0-500 m) at 22°N-25°N in summer (Fig. 11b).

The negative anomaly values of salinity near the surface reflect the seasonal displacement of the ITCZ in the western Atlantic. Due to large freshwater influx, negative contours of 0.35-0.55‰ are found in the 0-50m layers at the equator in spring and at 10°N in fall (Figs. 11a and 11c). The advection of subtropical salty water at the 100-200 m depth is clearly shown in summer in the northern subtropics, and in winter in the southern subtropics.

Although the contribution of salinity to density below 100 m depth in the tropical Atlantic is negligible compared to that of temperature, salinity substantially affects density in the mixed layer (Figs. 12a-d). Even in the layer, the contribution of temperature to density is 2-3 times larger than that of salinity (not shown). However, the effect of salinity to density change of 0.0035g/cm^3 for fall in the mixed layer in the ITCZ (5-10°N) is almost as much as that of temperature (Fig. 12c).

Simulation

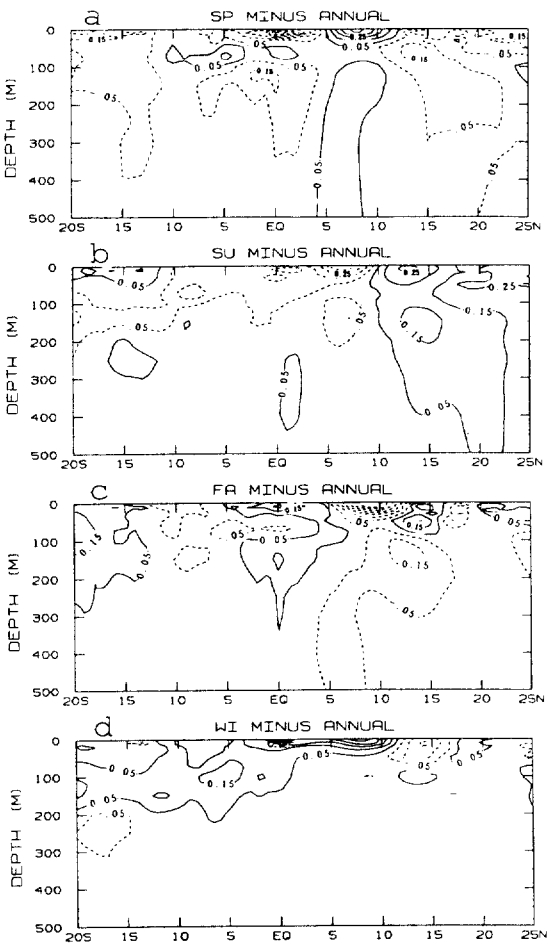

Fig. 11. Observed seasonal mean minus annual mean salinity (‰), zonally averaged in the region between 30°W and 50°W, as a function of latitude and depth for (a) spring, (b) summer, (c) fall, and (d) winter. The definition for seasons is the same as that of Fig. 1. Contour interval is 0.1‰, for instance, ±0.05, ±0.15, ±0.25···

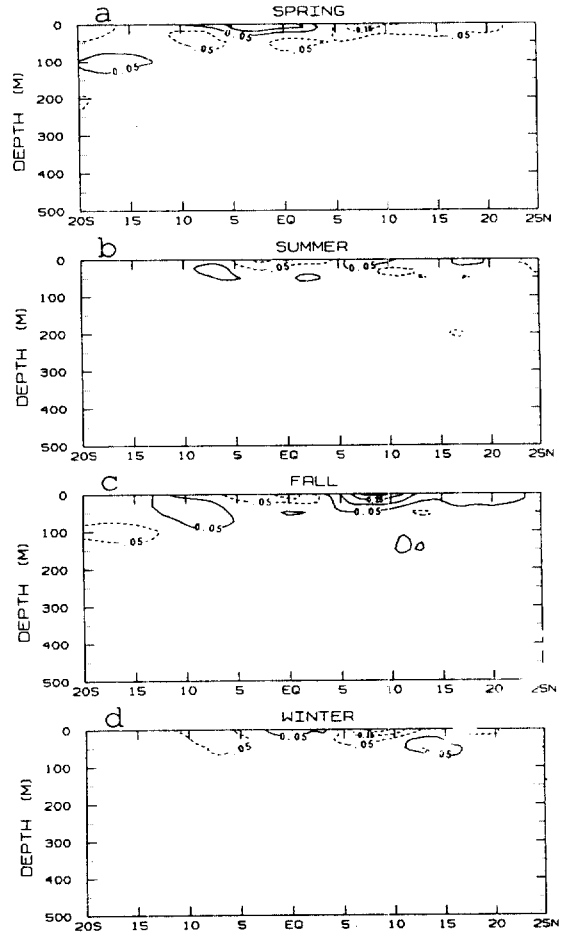

Fig. 12. Zonally averaged seasonal mean density $(\sigma_{S_a,T_P}-1)10^3$ minus seasonal mean density $(\sigma_{S,T_P}-1)10^3$ in the tropical Atlantic Ocean between South America coast and Africa coast as a function of latitude and depth for (a) spring, (b) summer, (c) fall, and (d) winter. Here S_a is observed annual salinity, and the T, S without subscript are observed seasonal temperature and salinity, respectively. Thus, the above difference between two density values represents the contribution of seasonal salinity to seasonal density. The definition for seasons is the same as that of Fig. 1. Contour interval is 0.1 g/cm^3, for instance, ±0.05, ±0.15, ±0.25···

We try to show the differences between model and observed zonally averaged seasonal salinity in the region between 30°W and 50°W (Figs. 13a-d). Model salinity values for all seasons in the area between 6°S and 10°N are systematically higher by maximum 0.8‰ than those of observed analysis. This occurs in the whole layer between surface and 500 m depth. On the other hand, model values are systematically lower by maximum −0.8‰ for four seasons in the subtropics of both hemispheres than those of observation. These negative values of the model minus observed salinity occur in the whole layer in the northern subtropics, while the negative values occur in the layer above 300 m depth in the southern subtropics.

The major disagreement between observed and simulated results comes from the fact that the simulated salinity is higher in the tropics but lower in the subtropics than the observed salinity. This

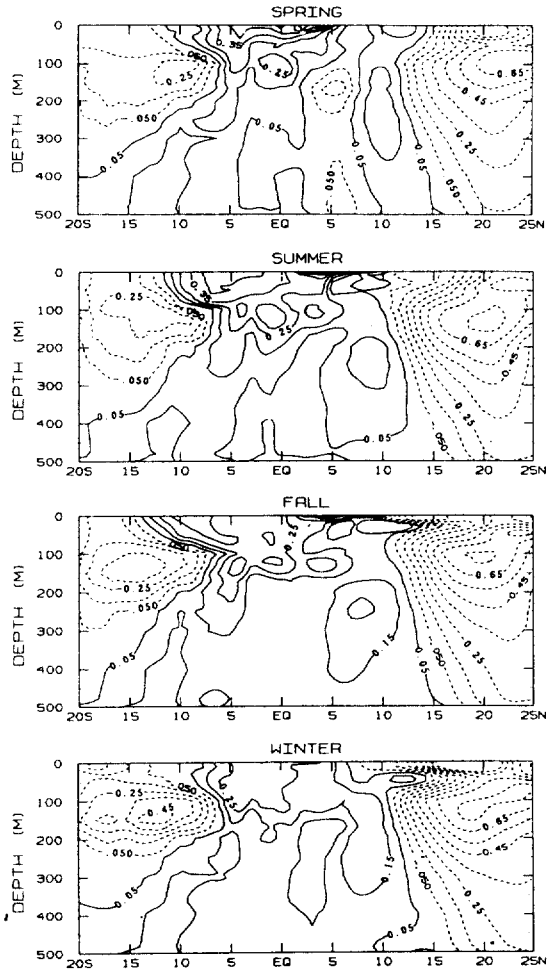

Fig. 13. As in Fig. 11 except for simulated seasonal mean minus observed seasonal mean salinity.

tendency in model leads to less salinity meridional gradients from the tropics to the subtropics than in observations. This may result from the stronger horizontal advection and mixing in model, and thus reduce the salt difference between the tropics and the subtropics.

Another source for the disagreement between observed and simulated transports is the freshwater budget which has driven the model as an input data. If the freshwater influx into the ocean is underestimated in the tropics and overestimated in the subtropics, the above result which systematically shows the less salinity gradients may happen (see also Figs. 8 and 13). Although in this case the effect due to the freshwater budget is anticipated to be most sensitive to upper ocean, for instance, mixed layer, it could deeply penetrate into the ocean, depending upon how efficient the vertical mixing is.

SUMMARY AND DISCUSSION

The distributions of seasonal salinity are obtained from both objectively analyzed historical (1900-86) salinity observations and an ocean general circulation model. Our observed salinity data in the surface, zonal and meridional fields are in reasonable agreement with other independent observations of Defant (1981) and Levitus (1982). However, the data in this study give more realistic seasonal features of salinity based on a longer climatological period, and more consistent patterns with temperature structure particularly in the NECC region. The pattern of sea surface salinity shows that heavy rainfall in the ITCZ directly relates with well-developed low salinity (<35.5‰) belt. The amplitude and phase analysis for the mixed-layer salinity suggests that two salinity masses, originated from different latitudinal areas, merge into 13~15°N zone.

The effect of salinity on density below 100 m depth in the tropical Atlantic is negligible compared to that of temperature, but salinity substantially affects density in the mixed layer. The contribution of temperature to density in the mixed layer is still 2~3 times larger than that of salinity. However, the effects of temperature and salinity are comparable for fall in the ITCZ (5-10°N).

We estimate the salinity in the tropical Atlantic from a multilevel primitive equation model. In the model the surface boundary conditions include surface hydrological forcing by rainfall, evaporation and river discharge. By comparing the salinity at the surface-500 m layer for observation and simulation, we examine the possibility of employing a sophisticated model over the observed data sparse region.

Recently Carton (1991) has estimated the indirect impact of net freshwater flux on sea surface temperature by comparing two numerical simulations, with and without surface freshwater forcing,

from the same model also used in the present study. The main discrepancy between observed and simulated salinity values, found in this current study, is the fact that the simulated one is systematically higher in the tropics but lower in the substropics than the observed one. This trend in the model results in less salinity meridional gradients from the tropics to the subtropics.

ACKNOWLEDGMENTS

Dr. Carton at University of Maryland has provided important assistance in making these calculations. Drs. Y.-Q. Kang and S.-K. Byun gave helpful comments on this manuscript. K.-O. Park and H.-J. Kim provided technical assistance with the preparation of the paper.

REFERENCES

Carton, J.A. 1991. Effect of seasonal surface freshwater flux on sea surface temperature in the tropical Atlantic Ocean. *J. Geophys. Res.*, **96**: 12593-12598.

Carton, J.A., and J. Shukla, 1991. Predictability of the tropical Atlantic Ocean. *J. Mar. Syst.*, **1**: 299-313.

Defant, A., 1936. Die Tropasphäre, Walter de Gruyter, Berlin. (English translation, The Troposphere, edited by W.J. Emery, Amerind, New Delhi, 1981. 113pp.).

Haltiner, G.J. and R.T. Williams, 1980. Numerical prediction and dynamic meteorology, John Wiley & Sons, New York, 356-365.

Hellerman, S., and M. Rosenstein, 1983. Normal monthly wind stress data over the world ocean with error estimates. *J. Phys. Oceanogr.*, **13**: 1093-1104.

Levitus, S., 1982. Climatological atlas of the world ocean, U.S. Dep. of Commer., Rockville, Md. NOAA Prof. Pap. 13: 174pp.

Levitus, S., 1986. Annual cycle of salinity and salt storage in the world ocean. *J. Phys. Oceanogr.*, **16**: 322-343.

Miller, J.R., 1976. The salinity effect in a mixed layer ocean model. *J. Phys. Oceanogr.*, **6**: 29-35.

Oberhuber, J.M., 1988. An atlas based on the "COADS" data set: The budgets of heat, buoyancy and turbulent kinetic energy at the surface of the global ocean, Rep. 15: Max-Planck-Inst. for Meteorol., Hamburg, Germany.

Pacanowski, R.C., and S.G.H. Philander, 1981. Parameterization of vertical mixing in numerical models of tropical oceans. *J. Phys. Oceanogr.*, **11**: 1443-1451.

Philander, S.G.H., and R.C. Pacanowski, 1986a. A model of the seasonal cycle of the tropical Atlantic Ocean. *J. Geophys. Res.*, **91**: 14192-14206.

Philander, S.G.H., and R.C. Pacanowski, 1986b. The mass and heat budget in a model of the tropical Atlantic Ocean. *J. Geophys. Res.*, **91**: 14212-14220.

UNESCO (United Nations Educational, Scientific, and Cultural Organization), 1969. Discharge of Selected Rivers of the World, vol. I: General and Regime Characteristics of Stations Selected, 70pp., Paris.

UNESCO, 1971a. Discharge of Selected Rivers of the World, vol. II: part I, Monthly and Annual Discharges Recorded at Various Selected Stations (From Start of Observations up to 1964), Paris, 194pp.

UNESCO, 1971b. Discharge of Selected Rivers of the World, vol. III: Mean Monthly and Extreme Discharges (1965-1969), Paris, 98pp.

UNESCO, 1978. World Water Balance and Water Resources of the Earth, Paris, 663pp.

UNESCO, 1979. Discharge of Selected Rivers of the World, vol. III: part III, Mean Monthly and Extreme Discharges (1972-1975), Paris, 104pp.

Yoo, J.-M., and J.A. Carton, 1988. Spatial dependence of the relationship between rainfall and outgoing longwave radiation in the tropical Atlantic. *J. Clim.*, **1**: 1047-1054.

Yoo, J.-M., and J.A. Carton, 1990. Annual and interannual variation of the freshwater budget in the tropical Atlantic Ocean and Caribbean Sea, *J. Phys. Oceanogr.*, **20**: 831-845.

Accepted December 3, 1992